Biosensors and Bioelectronics 139 (2019) 111335

Contents lists available at ScienceDirect

Biosensors and Bioelectronics

journal homepage: www.elsevier.com/locate/bios

Coordination polymers of Tb^{3+}/Nucleotide as smart chemical nose/tongue toward pattern-recognition-based and time-resolved fluorescence sensing

Xin-Yue Han, Qian-Xi Fan, Zi-Han Chen, Ling-Xue Deng, Zheng-Qi Fang, Guoyue Shi, Min Zhang*

School of Chemistry and Molecular Engineering, Shanghai Key Laboratory for Urban Ecological Processes and Eco-Restoration, East China Normal University, 500 Dongchuan Road, Shanghai, 200241, China

ARTICLE INFO

Keywords:
Time-resolved fluorescence
Lanthanide-based sensor array
Pattern recognition
Multiple analysis

ABSTRACT

The abundant functional groups on guanosine monophosphate (GMP) make it possible to interact with various metal ions. The subtle difference in the structure of GMP and deoxy-guanosine monophosphate (dGMP) coupled with Tb3+ can be readily exploited to form two coordination polymers, which have been unveiled as two time-resolved fluorescence (TRF) sensing reporters (Tb-GMP and Tb-dGMP) in our study. Based on this finding, herein, we have proposed a novel TRF orthogonal sensing array (Tb-GMP/dGMP) for pattern-recognition-based sensing of various metal ions. In addition, upon integration of some thiol-affinity metal ions, Tb-GMP/dGMP can be further extended to construct two metal ion-involved pattern-recognition-based sensor arrays (Tb-GMP/dGMP-Cu, Tb-GMP/dGMP-Ag) for the TRF sensing different levels of disease-relevant biothiols in biofluids, illustrating the powerful and multifunctional capabilities of the Tb-GMP/dGMP system and would inspire simpler and more widespread designs of chemical nose/tongue-based applications.

1. Introduction

The abnormal level of some biochemical substances (i.e. biomarkers) in biofluids would potentially indicate the occurrence of diseases (Sawyers, 2008; Chinen et al., 2015; Wu and Qu, 2015; Kim et al., 2017). For example, Wilson's disease could be confirmed by measuring aberrant contents of Cu^{2+} in urine (Sarkar, 1999), and the unusual concentration of homocysteine (Hcys) in urine is reported to correlate with homocystinuria (Wilson, 2002). The above cases only refer to one analyte to evaluate the potential risk regarding diseases, and have greatly promoted the development of analyte-specific biosensor in recent years (Frommer et al., 2009). However, some mental illnesses, such as Alzheimer's disease (AD) and Parkinson's disease (AD), have more and complex pathogenic analytes which make it difficult to achieve precise causes in time or perform any suitable treatments. Thus, It is appealing to develop multifunctional sensing systems that can promise the simultaneous sensing and differentiating of many analytes for practical clinical diagnosis.

One way to address this issue is to design chemical nose/tongue-mimic sensor arrays capable of the pattern-recognition-based differentiation of multiple analytes through certain sensor elements with principal component analysis (PCA) (Lin et al., 2018; Bigdeli et al., 2017; Tao et al., 2014). For example, Lik et al. reported that 6 oligodeoxyfluoroside-based organic fluorescent dyes can be used as a sensor array for differentiating and detecting 50 metal ions (Yuen et al., 2014). Although these organic fluorescent dye-involved sensor arrays have achieved impressive results, some disadvantages still occur, such as sophisticated syntheses, high costs and background signals being noticed without analytes. Thus, it is highly admirable to unveil simple, low-cost and reliable strategies for the development of novel chemical nose/tongue sensor arrays, e.g. in a label-free mix-and-detect format or a background-free mode. Recent years have witnessed the rapid progress of lanthanide-related time-resolved fluorescence (TRF) probes or sensors, in which unique spectroscopic properties (i.e. long fluorescence lifetime, large Stokes shifts, and sharp emission bands) of lanthanide-derived materials (e.g. lanthanide ions-nucleic acid complex) have been explored for the widespread applications regarding label-free and background-free TRF arrays (Zhang et al., 2013, 2014a, 2014b; Xue et al., 2016; Wang et al., 2017). More recently, we have first reported single-stranded DNA (ssDNA)-sensitized lanthanide ions (Tb^{3+} or Eu^{3+}) TRF sensor arrays for label-free yet multifunctional background-free sensing of largescale metal ions (Xue et al., 2018a), in which the abundant functional groups and multiple recognition sites on ssDNA provide various forms when binding with metal ions (Xue et al., 2018b). However, such ssDNA-sensitized lanthanide ions TRF sensor arrays usually need artificial screened ssDNA that relied on commercial time-consuming synthesis. While nucleotides (e.g. GMP: guanosine monophosphate and dGMP: deoxy-guanosine monophosphate), as basic

* Corresponding author.
E-mail address: mzhang@chem.ecnu.edu.cn (M. Zhang).

https://doi.org/10.1016/j.bios.2019.111335
Received 16 April 2019; Received in revised form 10 May 2019; Accepted 16 May 2019
Available online 18 May 2019
0956-5663/

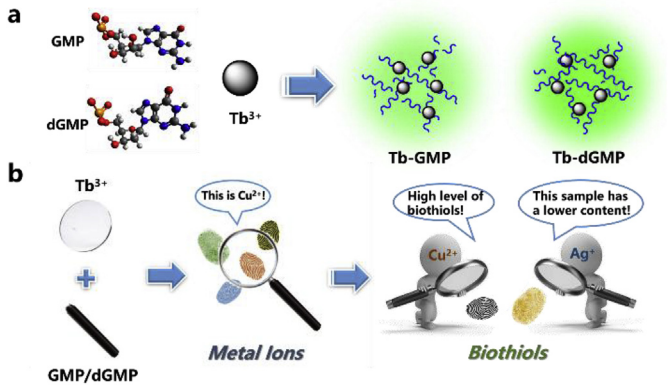

Scheme 1. Schematic illustration of the construction of Tb-GMP/dGMP sensor array and its pattern recognition of metal ions and biothiols.

units of DNA and RNA, are naturally abundant, and have multiple metal-recognizable sites, which can be utilized as potential candidates for distinguishing metal ions (Zhou et al., 2017). Additionally, nucleotides (such as GMP) can self-assemble with Tb^{3+} to form a supramolecular lanthanide coordination polymer (e.g. Tb-GMP), which have been used in many applications concerning biochemical analysis. Most of these applications require the encapsulation of heavy metal ions (Zhang et al., 2014b; Xue et al., 2016), fluorophores (Deng et al., 2015) or the nanomaterials (Zhang et al., 2016) to regulate the TRF properties of Tb^{3+} but scarcely focus on the different structure of nucleotides (e.g. GMP and dGMP, Fig. S1).

Enlighted by above facts, we herein propose a fundamentally novel orthogonal sensor array (Tb-GMP/dGMP) consisted of two lanthanide coordination polymers (Tb-GMP and Tb-dGMP) as TRF reporters, which can be readily employed for TRF pattern recognition of numerous metal ions in a label-free mix-and-detect and background-free format (Scheme 1). By addition of some Alzheimer's disease-related metal ions (Cu^{2+}, Fe^{3+} and/or Zn^{2+}) into artificial cerebrospinal fluid (aCSF), we have also successfully demonstrated that our proposed Tb-GMP/dGMP sensor array shows a powerful discrimination of multiple metal ions in biofluids toward the potential applications in the diagnosis of metal ion-involved diseases. Considering that some metal ions (e.g. Cu^{2+}, Ag^{+}) have different affinities toward biothiols (such as Cys: cysteine). Moreover, inspired by the opposite changes of TRF intensity in Tb-GMP/dGMP sensor array induced by Cu^{2+} in Tris-HCl buffer and Ag^{+} in Tris-HAc buffer, we have further constructed two metal ion-involved pattern-recognition-based assays (Tb-GMP/dGMP-Cu, Tb-GMP/dGMP-Ag) toward dynamic ranges of biothiols, which could be applied to macro-analysis of biothiols in urine and trace-analysis of biothiols related to redox balance in cerebrospinal fluid. Because of its appealing features, our Tb-GMP/dGMP system promises a multifunctional sensor array and would boost simpler and smarter design of chemical nose/tongue-mimic platforms.

2. Materials and methods

2.1. Materials and instruments

The following metal salts, NaCl, LiCl, KCl, $MgCl_2$, $CaCl_2$, $CuCl_2$, $PbCl_2$, $CoCl_2$, $ZnCl_2$, $CdCl_2$, $FeCl_2$, $FeCl_3$, $NiCl_2$, $AgNO_3$, $AlCl_3$, $MnCl_2$, $CrCl_3$, K_2CrO_4, $Hg(Ac)_2$, $HAuCl_4$ and $Pd(NO_3)_2$ were reagent grade and purchased from Sinopharm Chemical Reagent Co. Ltd. (Shanghai, China). $Tb(NO_3)_3$ were purchased from Diyang Chemical Co. Ltd. (Shanghai, China). Reduced glutathione (GSH), cysteine (Cys) and homocysteine (Hcys) were purchased from Sigma−Aldrich (St. Louis, MO). Guanosine monophosphate (GMP) and deoxy-guanosine monophosphate (dGMP) were commercially available from Sangon Inc. (Shanghai, China). Tris-HCl buffer and Tris-HAc buffer (100 mM, pH 7.4) was prepared using metal-free reagents in distilled water.

Fluorescence spectra were recorded by a microplate reader (infinite M200 pro, TECAN, Switzerland) using a black 384-well microplate (Corning, U.S.A.). The excitation wavelength used was 280 nm for the emission spectra. For the time-resolved fluorescence (TRF) spectra, a delay time of 50 μs and a counting time of 2 ms were used. The spectra of fluorescence lifetime were measured by using FLS980 Fluorescence Spectrometer (Edinburgh Instruments Ltd, UK). The Fourier transform infrared spectroscopy (FTIR) spectra were obtained with a Nicolet optical bench (Nexus 670).

2.2. Preparation of sensor arrays

Solution of $Tb(NO_3)_3$ (800 μM) and GMP or dGMP (800 μM) were mixed and incubated in Tris-HCl buffer (10 mM, pH 7.4) for 15 min as two reporters to construct the Tb-GMP/dGMP sensor array for the pattern recognition of metal ions including alkali metal, alkali earth metal, transition metal and so on. Tb-GMP/dGMP sensor array was then mixed Cu^{2+} (20 μM) in Tris-HCl buffer to form the Tb-GMP/dGMP-Cu sensor array for the pattern recognition of biothiols including GSH, Cys and Hcys. Additionally, changing Tris-HCl buffer to Tris-HAc buffer for eliminating the effect on Ag^{+} from Cl^{-}, another Tb-GMP/dGMP-Ag sensor array (20 μM Ag^{+} used) can be also built for the pattern recognition of biothiols indicated. All process mentioned above was conducted under room temperature.

2.3. Preparation of artificial biofluids

Artificial urine solution contained 170 mM urea, 1.1 mM lactic acid, 2.0 mM citric acid, 2.5 mM $CaCl_2$, 2.0 mM $MgSO_4$, 90 mM NaCl, 10 mM Na_2SO_4, 25 mM $NaHCO_3$, 7.0 mM KH_2PO_4, 7.0 mM K_2HPO_4, and 25 mM NH_4Cl which were all mixed in distilled water. Artificial cerebrospinal fluid (aCSF) was prepared by mixing 126 mM NaCl, 0.85 mM $MgCl_2$, 2.4 mM KCl, 1.1 mM $CaCl_2$, 27.5 mM $NaHCO_3$, 0.5 mM Na_2SO_4 and 0.5 mM KH_2PO_4 into distilled water. The pH of all solutions were adjusted to 7.4 by the addition of 1.0 M HCl.

2.4. Data analysis

SPSS 23.0 software (IBM) was used to perform principal component analysis (PCA). The data plotting was carried out with GraphPad Prism 7.0 software (San Diego, CA). Each sample was repeated in quintuplicate.

3. Result and discussion

3.1. Design of Tb-GMP/dGMP sensor array

Tb^{3+} alone is very poor at absorbing light due to its Laporte-forbidden f−f transitions, so direct excitation of Tb^{3+} to fluoresce is typically difficult (Zhang et al., 2013). Guanine (G) can greatly enhance the Tb^{3+} emission because its triplet energy state overlaps with the resonance energy levels of Tb^{3+} (Chatterji, 1988). It is reported that GMP can self-assemble with Tb^{3+} to form a supramolecular lanthanide coordination polymer (Tb-GMP), which can emit intense green fluorescence of Tb^{3+} due to energy transfer from G base to the emissive $^5D_4$ state of Tb^{3+} (Nishiyabu et al., 2009).

In this work, coordination polymers of Tb-GMP and Tb/dGMP were respectively prepared in a one-pot format. TEM images showed their typical network structures (Fig. 1a and b), proving the successful synthesis of Tb-GMP and Tb-dGMP. FTIR spectra of Tb-GMP and Tb/dGMP also indicated that Tb^{3+} successfully coordinated with GMP and dGMP (Fig. S2). As depicted in Fig. 1c, Tb-GMP and Tb-dGMP showed a sharp excitation peak at around 280 nm and exhibited emission at 546 nm due to the GMP or dGMP-sensitized fluorescence of Tb^{3+}, while Tb-dGMP (blue line) showed stronger fluorescence intensity than Tb-

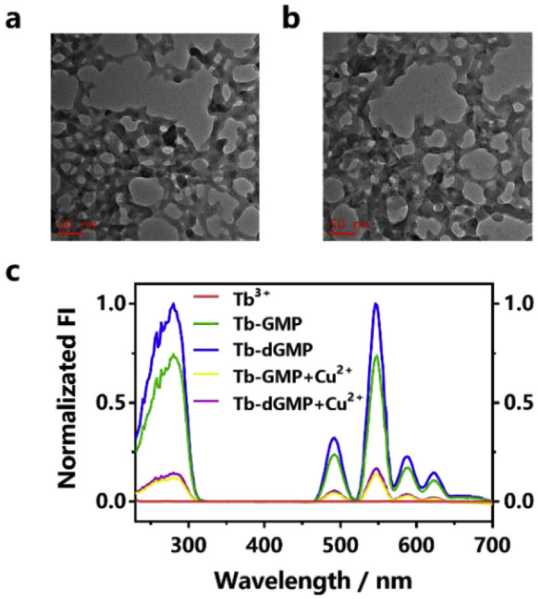

Fig. 1. TEM images of (a) Tb-GMP and (b) Tb-dGMP. (c) Excitation spectra and emission spectra of Tb^{3+} (red line), Tb-GMP (green line), Tb-dGMP (blue line), Tb-GMP + Cu^{2+} (yellow line) and Tb-dGMP + Cu^{2+} (purple line). (For interpretation of the references to colour in this figure legend, the reader is referred to the Web version of this article.)

GMP (green line). Upon the addition of Cu^{2+} to Tb-GMP and Tb-dGMP, their fluorescence peaks were quenched with varied degree (yellow line and purple line), which can be attributed to the differentiated interactions of Cu^{2+}/GMP and Cu^{2+}/dGMP for tuning the sensitization indicated above. The afore-said results can be also verified by the following fluorescence lifetime measurements (Fig. S3). The fluorescence lifetime of Tb-dGMP is 132.5 μs, which is longer than that of Tb-GMP (132.0 μs) and markedly longer than that of Tb^{3+} (118.3 μs). Moreover, there are discriminating fluorescence lifetime between Tb-GMP + Cu^{2+} (120.0 μs) and Tb-dGMP + Cu^{2+} (120.8 μs). The as-prepared Tb-GMP and Tb-dGMP with long-lifetime fluorescence can be readily employed as novel label-free TRF sensors for biochemical applications in a mix-and-detect and background-free format. There exist abundant functional groups in GMP or dGMP, which would provide excellent cites for the coordination with metal ions. At first, as a proof of concept, a label-free TRF sensor array (Tb-GMP/dGMP) can be thus developed for pattern recognition of metal ions. Upon challenged with metal ions, due to the different coordination affinity of GMP or dGMP toward metal ions, the selected sensors would show differentiable TRF changes and provide distinct responses to a variety of metal ions to realize their pattern recognition. Some metal ions (e.g. Cu^{2+}, Ag^{+}) can react with thiol (-SH) and other groups of biothiols (Cys, Hcys, and etc.), and there are distinct affinities between these metal ions and biothiols (Xue et al., 2018b). In the presence of biothiols, the strong affinity between Cu^{2+} (or Ag^{+}) and biothiols could prevent Cu^{2+} (or Ag^{+}) from binding Tb-GMP/dGMP, therefore the TRF properties of Tb-GMP/dGMP would be changed to a certain degree. Based on this fact, a new group of sensor arrays (i.e. Tb-GMP/dGMP-Cu, and Tb-GMP/dGMP-Ag) can be further constructed from the combination of Tb-GMP/dGMP and Cu^{2+} (or Ag^{+}) for the pattern recognition of biothiols.

3.2. Pattern-recognition-based TRF assay to metal ions using Tb-GMP/dGMP sensor array

To evaluate the discrimination ability of our proposed Tb-GMP/dGMP sensor array, 19 metal ions including some alkaline metal ions (Li^{+}, Na^{+}, K^{+}), alkaline-earth metal ions (Mg^{2+}, Ca^{2+}) and transition metal ions (Cr^{3+}, Mn^{2+}, Fe^{2+}, Fe^{3+}, Co^{2+}, Ni^{2+}, Cu^{2+}, Zn^{2+}, Ag^{+}, Cd^{2+}, Hg^{2+}, Au^{3+}, Pd^{2+}) were chosen as analytes (each at 50 μM). Each TRF response for a given metal ion was separately tested with Tb-GMP/dGMP sensor array (Tb-GMP, and Tb-dGMP), and the resultant TRF responses were recorded for generating pattern F/F_0 data (Fig. 2a) and the corresponding heat map (Fig. 2b). PCA was then utilized by calculating orthogonal eigenvectors (principal components, PC) that lie in the direction of the maximum variance within that data set to shorten the dimensionality of a data set for easier interpretation [24]. Thus, the PCA focuses the most significant characteristics (variance) of the data into a lower dimensional space. For the PCA, a TRF response matrix consisting of 2 Tb-GMP/dGMP sensors × 19 metal ions × 5 replicates was formed to generate canonical factors (98.87 and 1.13%). The most significant factors are plotted in 2D (Fig. 2c). Except the clusters of Na^{+}, K^{+}, and Mg^{2+} are slightly overlapped, those analytes produce various TRF patterns separately grouped in different clusters. Such results confirm that Tb-GMP/dGMP sensor array can act as a chemical nose/tongue, possessing powerful discrimination ability for sensing largescale metal ions.

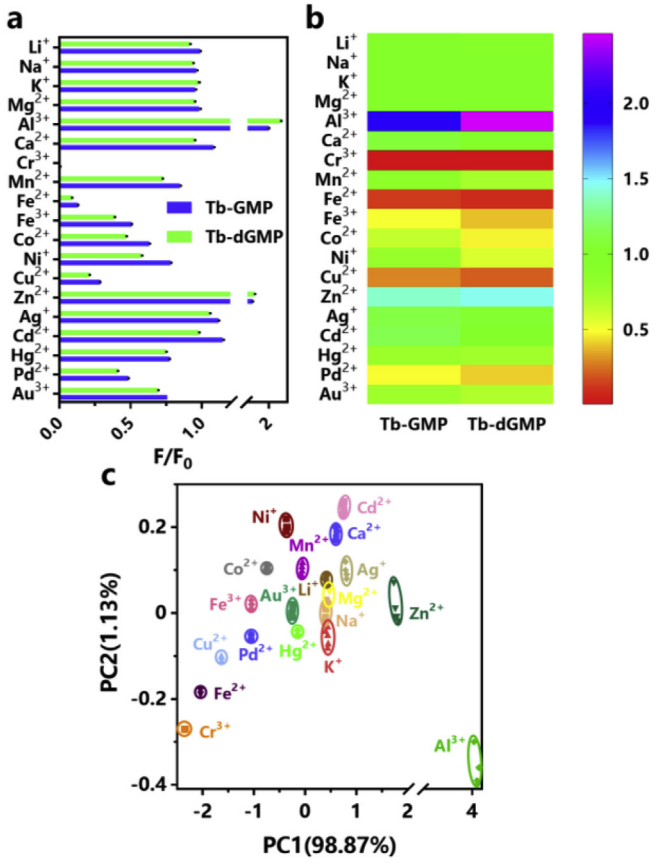

Fig. 2. (a) TRF response patterns of Tb-GMP/dGMP sensor array toward 19 metal ions (50 μM). (b) Heat map derived from TRF response patterns of Tb-GMP/dGMP sensor array toward metal ions indicated. (c) 2D canonical score plot for the presented sensor array against metal ions indicated.

To test the sensitivity of Tb-GMP/dGMP sensor array, four metal ions (Cu^{2+}, Al^{3+}, Hg^{2+}, and Cr^{3+}) were respectively picked to assess their analytical performances (Fig. 3 and Fig. S4). It can be noticed that for each metal ion, the PCA plots for various concentrations were followed certain patterns, and can be distinguished from each other at diverse concentrations. More interesting, Cu^{2+}, Cr^{3+} and Hg^{2+} display concentration-dependent quenching effects on TRF of Tb-GMP/dGMP sensor array (Fig. 3e, g, and h), while Al^{3+} results in a concentration-dependent enhancement effect (Fig. 3f). The combination of Tb^{3+} and GMP or dGMP are mainly based on guanine (G) and phosphate group (P). Additionally, Cu^{2+} is known for strong binding with G (Wang et al.,

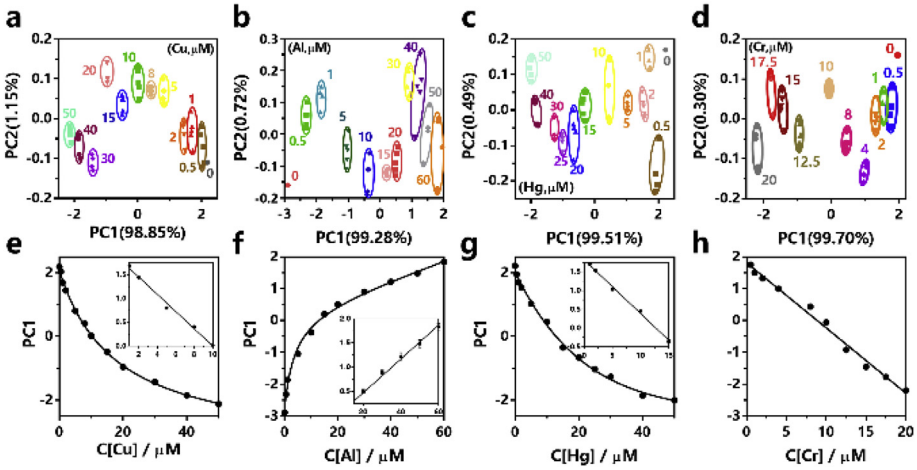

Fig. 3. (a, b, c, d) Canonical score plots, and (e, f, g, h) Plots of PC1 of Tb-GMP/dGMP sensor array toward varied concentrations of Cu^{2+} (0.5–50 μM), Al^{3+} (0.5–60 μM), Hg^{2+} (0.5–50 μM) and Cr^{3+} (0.5–20 μM), respectively.

2012), leading to the replacement of Tb^{3+} and thus reduce its TRF intensity. Likewise, Cr^{3+} can bind to the N7 of G and then be chelated by a nearby phosphate (Arakawa et al., 2000), and the apparent binding affinity to Cr^{3+} follows the order of G > C > A ≈ T (Zhou et al., 2016). Hg^{2+} can complex with GMP or dGMP via the amino group of the G moiety and the phosphate group, and Hg^{2+} is known to be an efficient fluorescence quencher (Zhang et al., 2014a,b). Al^{3+} has high density of positive charge and small ionic radius for inducing Tb-GMP/dGMP to form a specific complex, promoting the TRF enhancement in Tb-GMP/dGMP sensor array based on the HSAB principle (Izatt et al., 1971; Loo et al., 2010). Since PC2 (the second discriminant factor) was not exceeding 40%, PC1 (the first discriminant factor) can be used to quantify the concentrations of metal ions (Xue et al., 2018a). As shown in Fig. 3e–h, this Tb-GMP/dGMP sensor array was sensitive to detect different concentrations of these metal ions.

After successful pattern recognition of various levels of metal ions, we also examined the recognition ability of Tb-GMP/dGMP sensor array toward a set of mixtures of Cu^{2+} and Zn^{2+} (Cu^{2+}:Zn^{2}), Hg^{2+} and Cd^{3+} (Hg^{2+}:Cd^{2+}), and Cr^{3+} and Mn^{2+} (Cr^{3+}:Mn^{2+}) with different molar ratios. We detected the TRF responses of Tb-GMP/dGMP sensor array toward these mixtures (Fig. S5), and these mixtures were characteristically distinguished from each other in PCA plots and properly located with the order of molar ratios (Fig. 4a–c). Seeing that PC2 of the PCA plots was < 40%, it was acceptable to apply PC1 to profile the pattern of the mixture samples. Fig. 4f–h showed that Tb-GMP/dGMP sensor array can be fully sensitive for mapping these metal ions in predetermined mixtures for tracing each metal ion alone.

Thereafter, we proved the sensitivity of Tb-GMP/dGMP sensor array to metal ions' valence states (Fig. 4 and Fig. S5). The mixtures of two valence states of Cr (Cr^{3+}:Cr^{6+}) and Fe (Fe^{3+}:Fe^{2+}) can be completely differentiated from each other in the PCA plots (Fig. 4d–e). The resultant PC1 from the PCA plots of Tb-GMP/dGMP sensor array can also describe the pattern of the tested samples (Cr^{3+}:Cr^{6+} and Fe^{3+}:Fe^{2+}), and effectively locate/match these metal ions at various mixtures for determining each metal ion in them (Fig. 4i–j). Those results confirmed that this system would be potentially suitable for sensitive analysis of complex composition.

Precise recognition and confirmation of metal ion-related diseases such as AD are meaningful toward healthcare monitoring. Several metal ions (e.g. Cu^{2+}, Zn^{2+}, and Fe^{3+}) are correlated with AD due to their participation in important metabolic or biochemical processes (Ayton et al., 2015). The simultaneous sensing and differentiating of these metal ions for potential clinical diagnosis of AD in biofluids (e.g. CSF) was further demonstrated using Tb-GMP/dGMP sensor array (Fig. 5 and Fig. S6). We prepared three group of biofluid-relevant samples by spiking different concentrations of Cu^{2+} (i.e. single analyte), Cu^{2+}:Zn^{2+} (i.e. two analytes) at different molar ratios, and Cu^{2+}:Zn^{2+}:Fe^{3+} (i.e. three analytes) at various molar ratios to aCSF. As depicted in Fig. 5, these samples in aCSF were fully separated from each other in PCA plots and properly arranged with the concentrations and the order of molar ratios in addressable tracks. Moreover, Tb-GMP/dGMP sensor array can be feasibly employed for the simultaneous determination of Cu^{2+} and Zn^{2+} in urine samples related to Wilson's disease [31] (Fig. S7).

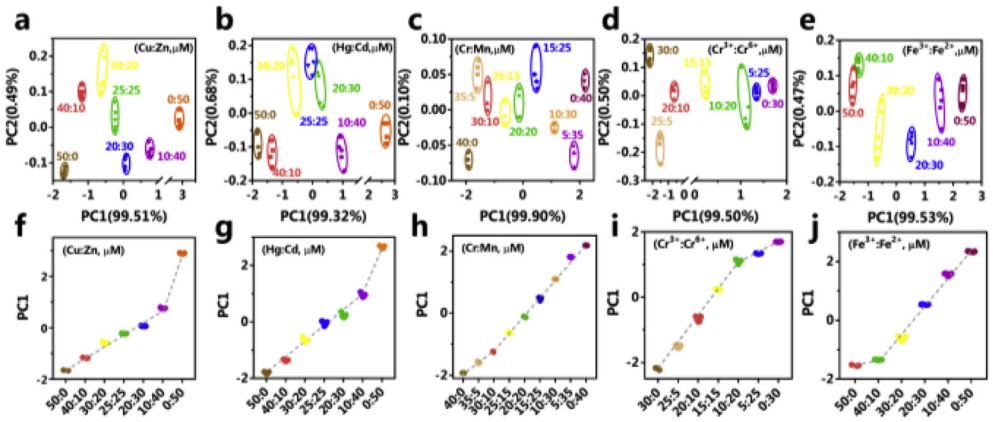

Fig. 4. Canonical score plots and plots of PC1 of Tb-GMP/dGMP sensor array toward different molar ratios of (a, f) Cu^{2+}:Zn^{2+} (50:0, 40:10, 30:20, 25:25, 20:30, 10:40 and 0:50, all for μM), (b, g) Hg^{2+}:Cd^{2+} (50:0, 40:10, 30:20, 25:25, 20:30, 10:40 and 0:50, all for μM), (c, h) Cr^{3+}:Mn^{2+} (40:0, 35:5, 30:10, 25:15, 20:20, 15:25, 10:30, 5:35 and 0:40, all for μM), (d, i) Cr^{3+}:Cr^{6+} (30:0, 25:5, 20:10, 15:15, 10:20, 5:25 and 0:30, all for μM) and (e, j) Fe^{3+}:Fe^{2+} (50:0, 40:10, 30:20, 20:30, 10:40 and 0:50, all for μM), respectively.

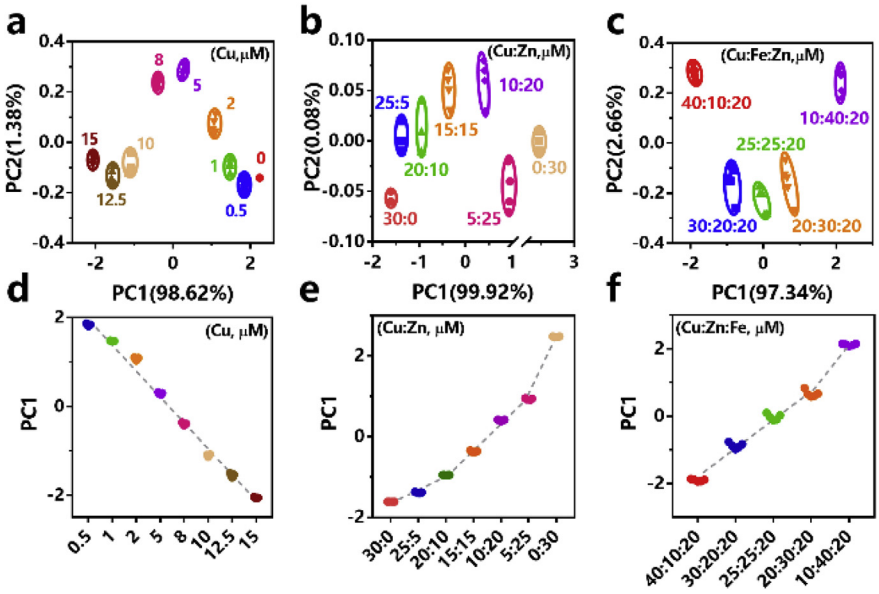

Fig. 5. (a, b, c) Canonical score plots, and (d, e, f) Plots of PC1 of Tb-GMP/dGMP sensor array toward different concentration of Cu^{2+} (0.5–15 μM), and different molar ratios of Cu^{2+}:Zn^{2+} (30:0, 25:5, 20:10, 15:15, 10:20, 5:25 and 0:30, all for μM) and Cu^{2+}:Zn^{2+}:Fe^{3+} (40:10:20, 30:20:20, 25:25:20, 20:30:20 and 10:40:20, all for μM) in aCSF.

3.3. Assays to biothiols using Tb-GMP/dGMP-Cu or Tb-GMP/dGMP-Ag sensor arrays

Apart from monitoring metal ions, Tb-GMP/dGMP sensor array can combine certain metal ions to develop the ensemble of Tb-GMP/dGMP and metal ions for further distinguishing targets capable of strongly binding to the metal ions used. As discussed above, biothiols, a group of important biochemical compounds, can be thus selected as such model targets based on their specific reactivity with some metal ions (e.g., Cu^{2+} and Ag^{+}). Upon the presence of Cu^{2+}, Tb-GMP/dGMP sensor array showed distinct TRF-quenching responses to Cu^{2+} in Tris-HCl buffer (Fig. 2a and b). Our previous work revealed that Ag^{+} can strongly enhance the TRF of G-rich DNA-sensitized Tb^{3+} (Chen et al., 2019). However, due to Cl^{-} in Tris-HCl buffer (100 mM, pH = 7.4) used, Ag^{+} may be shielded and no obvious TRF enhancement of Tb^{3+} was observed in the copolymers of Tb/GMP or Tb/dGMP (Fig. 2). When switching to Tris-HAc buffer (100 mM, pH = 7.4), the copolymers of Tb/GMP or Tb/dGMP emerged Ag^{+}-dependent significant and differentiated TRF-enhancing responses (Fig. S8).

Both Cu^{2+} and Ag^{+} can coordinate with thiol (-SH) and other groups of biothiols (Cys, Hcys, and GSH) with distinct affinities (Xue et al., 2018b). Upon the addition of biothiols, the strong affinity between Cu^{2+} (or Ag^{+}) and biothiols could prevent Cu^{2+} (or Ag^{+}) from binding Tb-GMP/dGMP, the TRF properties of Tb-GMP/dGMP would be therefore altered with various patterns. Based on the above facts, two types of sensor arrays for pattern recognition of biothiols were then proposed, one is Tb-GMP/dGMP-Cu in Tris-HCl buffer, and the other is Tb-GMP/dGMP-Ag in Tris-HAc buffer. As revealed in Figs. S9a and S9b, the TRF response patterns of Tb-GMP/dGMP-Cu sensor array in Tris-HCl buffer toward biothiols (Cys, Hcys, and GSH) are differentiable, ensuring its feasibility for pattern recognition of biothiols via PCA. For each biothiol, TRF responses against the sensor array were parallelly tested five times, generating a matrix of 2 sensors × 3 thiols × 5 replicates. For PCA, these biothiols were fully discriminated with high identification accuracy (Fig. S9c). Similar results regarding pattern recognition of biothiols can be realized using Tb-GMP/dGMP-Ag sensor array in Tris-HAc buffer (Figs. S9d–S9f). To verify the possibility of constructing sensor arrays with other metal ions for identifying thiols, we further realized the pattern recognition of three biothiols (GSH, Cys and Hcys, all in 50 μM) in consideration of the formation of strong complex mediated by Au^{3+} or Pd^{2+} (Fig. S10), which proved the abundant design based on Tb-GMP/dGMP. However, in this work, we rather chose Cu^{2+} and Ag^{+} for the economy price and low toxicity to design facile biothiol-pattern-recognition sensor arrays which also showed contrary formats as “turn-on” and “turn-off”.

Different concentrations of GSH, Cys, and Hcys were then selected to investigate the analytical performances of our proposed Tb-GMP/dGMP-Cu sensor array (Fig. S11) and Tb-GMP/dGMP-Ag sensor array (Fig. S12). From the results, various concentrations of 3 biothiols can be effectively distinguished into different clusters, proving that our sensor arrays are robust for the TRF pattern recognition of multiple biothiols (Figs. S11 and S12). With a series of biothiols successfully discriminated, the mixtures of biothiols (GSH + Cys, GSH + Hcys) with different molar ratios were adopted to respectively challenge Tb-GMP/dGMP-Cu sensor array and Tb-GMP/dGMP-Ag sensor array for discriminating the coexisting biothiols. As shown in Fig. 6, these mixtures were fully separated from each other in the PCA plots and arranged with the order of molar ratios.

Biothiols are common with neurodegenerative diseases, in which the concentrations of biothiols are different (Luo et al., 2015; Deng et al., 2013; Han et al., 2018). It is desirable for health monitoring to dynamically monitoring multiple biothiols in biofluids. Thus, the recognition ability of Tb-GMP/dGMP-Cu sensor array and Tb-GMP/dGMP-Ag sensor array were further examined toward a set of mixtures of biothiols with different molar ratios in biofluids (Figs. S13 and S14), in this study, different combinations of GSH + Cys (70 + 0, 60 + 10, 50 + 20, 40 + 30, 30 + 40, 20 + 50, 10 + 60, 0 + 70, all in μM) were prepared in artificial urine and GSH + Hcys (20 + 0, 12.5 + 7.5, 10:10, 5:15, 2.5 + 17.5, 0 + 20, all in μM) were prepared in artificial cerebrospinal fluid. From Figs. S13 and S14, such Tb-GMP/dGMP-Cu and Tb-GMP/dGMP-Ag sensor arrays can be potentially extended for the pattern analysis of multiple biothiols in biofluids.

4. Conclusion

In summary, the first practical invention of coordination polymers of Tb^{3+}/nucleotide-based sensor array has been introduced for pattern recognition of multiple analytes in a label-free mix-and-detect and background-free format. In our study, we focused on the subtle difference in the structure of guanosine monophosphate (GMP) and deoxyguanosine monophosphate (dGMP). Two coordination polymers of Tb-GMP and Tb-dGMP have been formed and unveiled as two time-resolved fluorescence (TRF) sensing reporters, which can be successfully employed as a chemical nose/tongue-mimic sensor array (i.e. Tb-GMP/dGMP) for TRF pattern recognition of largescale metal ions based on the different coordination affinity of GMP or dGMP toward metal ions.

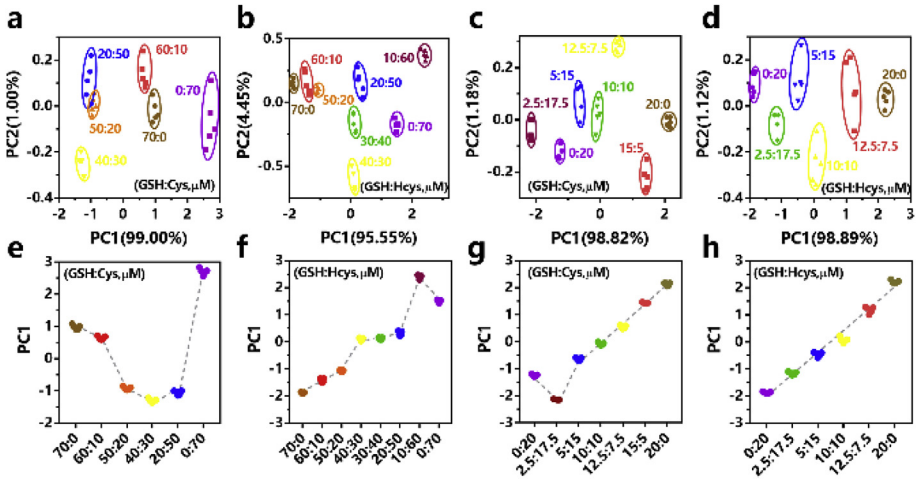

Fig. 6. (a, b, c, d) Canonical score plots, and (e, f, g, h) Plots of PC1 of Tb-GMP/dGMP-Cu sensor array toward different molar ratio of GSH:Cys (70:0, 60:10, 50:20, 40:30, 20:50 and 0:70, all for μM) and GSH:Hcys (70:0, 60:10, 50:20, 40:30, 30:40, 20:50, 10:60 and 0:70, all for μM), and Tb-GMP/dGMP-Ag sensor array toward different molar ratio of GSH:Cys (20:0, 15:5, 12.5:7.5, 10:10, 5:15, 2.5:17.5 and 0:20, all for μM) and GSH:Hcys (20:0, 12.5:7.5, 10:10, 5:15, 2.5:17.5 and 0:20, all for μM), respectively.

Furthermore, the ensemble of Tb-GMP/dGMP sensor array and certain metal ions (Tb-GMP/dGMP-Cu and Tb-GMP/dGMP-Ag) in different buffers have been shown to be another TRF pattern sensing systems for differentiation of diverse biothiols with high sensitivity and selectivity. Moreover, our proposed sensor arrays also show good anti-interference performance in complex media, such as artificial cerebrospinal fluid. We believe that the present study will broaden the scope of lanthanide/nucleotide-related research and inspire more development of chemical nose/tongue-mimic multifunctional sensing platforms.

Declaration of interests

The authors declare that they have no known competing financial interests or personal relationships that could have appeared to influence the work reported in this paper.

CRediT authorship contribution statement

Xin-Yue Han: Investigation, Formal analysis, Writing - review & editing. **Qian-Xi Fan:** Writing - review & editing. **Zi-Han Chen:** Writing - review & editing. **Ling-Xue Deng:** Writing - review & editing. **Zheng-Qi Fang:** Writing - review & editing. **Guoyue Shi:** Writing - review & editing. **Min Zhang:** Investigation, Writing - review & editing.

Acknowledgments

This work was supported by the National Natural Science Foundation of China (Nos. 21775044, 21675053, 21635003) and Key Project of the Shanghai Science and Technology Committee (No. 18DZ1112700).

Appendix A. Supplementary data

Supplementary data to this article can be found online at https://doi.org/10.1016/j.bios.2019.111335.

References

Arakawa, H., Ahmad, R., Naoui, M., Tajmir-Riahi, H.A., 2000. J. Biol. Chem. 275, 10150–10153.
Ayton, S., Lei, P., Bush, A.I., 2015. Neurotherapeutics 12, 109–120.
Bigdeli, A., Ghasemi, F., Golmohammadi, H., Abbasi-Moayed, S., Nejad, M.A.F., Fahimi-Kashani, N., Jafarinejad, S., Hormozi-Nezhad, M.R., 2017. Nanoscale 9, 16546–16563.
Chatterji, D., 1988. Biopolymers 27, 1183–1186.
Chen, Z.H., Han, X.Y., Deng, L.X., Lin, Z.Y., Mu, F.Y., Zhang, S., Shi, G., Zhang, M., 2019. Talanta 191, 235–240.
Chinen, A.B., Guan, C.M., Ferrer, J.R., Barnaby, S.N., Merkel, T.J., Merkin, C.A., 2015. Chem. Rev. 19, 10530–10574.
Deng, J., Jiang, Q., Wang, Y., Yang, L., Yu, P., Mao, L., 2013. Anal. Chem. 85, 9409–9415.
Deng, J., Yu, P., Wang, Y., Mao, L., 2015. Anal. Chem. 87, 3080–3086.
Frommer, W.B., Davidson, M.W., Campbell, R.E., 2009. Chem. Soc. Rev. 38, 2833–2841.
Han, X.Y., Chen, Z.H., Zeng, J.Z., Fan, Q.X., Fang, Z.Q., Shi, G., Zhang, M., 2018. ACS Appl. Mater. Interfaces 10, 31725–31734.
Izatt, R.M., Christensen, J.J., Rytting, J.H., 1971. Chem. Rev. 71, 439–482.
Kim, S.J., Choi, S.J., Jang, J.S., Cho, H.J., Kim, I.D., 2017. Acc. Chem. Res. 50, 1587–1596.
Lin, Z.Y., Xue, S.F., Chen, Z.H., Han, X.Y., Shi, G., Zhang, M., 2018. Anal. Chem. 90, 8248–8253.
Loo, K., Degtyareva, N., Park, J., Sengupta, B., Reddish, M., Rogers, C.C., Bryant, A., Petty, J.T., 2010. J. Phys. Chem. B 114, 4320–4326.
Luo, Y., Zhang, L., Liu, W., Yu, Y., Tian, Y., 2015. Angew. Chem. Int. Ed. 54, 14053–14056.
Nishiyabu, R., Hashimoto, N., Cho, T., Watanabe, K., Yasunaga, T., Endo, A., Kaneko, K., Niidome, T., Murata, M., Adachi, C., Katayama, Y., Hashizume, M., Kimizuka, N., 2009. J. Am. Soc. Chem. 131, 2151–2158.
Sarkar, B., 1999. Chem. Rev. 99, 2535–2544.
Sawyers, C.L., 2008. Nature 452, 548–552.
Tao, Y., Ran, X., Ren, J., Qu, X., 2014. Small 10, 3667–3671.
Wang, C., Li, Y., Jia, G., Liu, Y., Lu, S., Li, C., 2012. Chem. Commun. 48, 6232–6234.
Wang, Q.X., Xue, S.F., Chen, Z.H., Ma, S.H., Zhang, S., Shi, G., Zhang, M., 2017. Biosens. Bioelectron. 94, 388–393.
Wilson, P.W.F., 2002. J. Am. Med. Assoc. 288, 2042–2043.
Wu, L., Qu, X., 2015. Chem. Soc. Rev. 44, 2963–2997.
Xue, S.F., Lu, L.F., Wang, Q.X., Zhang, S., Zhang, M., Shi, G., 2016. Talanta 158, 208–213.
Xue, S.F., Chen, Z.H., Han, X.Y., Lin, Z.Y., Wang, Q.X., Shi, G., Zhang, M., 2018a. Anal. Chem. 90, 3443–3451.
Xue, S.F., Han, X.Y., Chen, Z.H., Yan, Q., Lin, Z.Y., Shi, G., Zhang, M., 2018b. Anal. Chem. 90, 10614–10620.
Yuen, L.H., Franzini, R.M., Tan, S.S., Kool, E.T., 2014. J. Am. Chem. Soc. 136, 14576–14582.
Zhang, M., Le, H.N., Jiang, X.Q., Yin, B.C., Ye, B.C., 2013. Anal. Chem. 83, 11665–11674.
Zhang, M., Qu, Z.B., Ma, H.Y., Zhou, T., Shi, G., 2014a. Chem. Commun. 50, 4677–4679.
Zhang, M., Qu, Z. b., Han, C.M., Lu, L.F., Li, Y.Y., Zhou, T., Shi, G., 2014b. Chem. Commun. 50, 12855–12858.
Zhang, X., Deng, J., Xue, Y., Shi, G., Zhou, T., 2016. Environ. Sci. Technol. 50, 847–855.
Zhou, W., Yu, T., Vazin, M., Ding, J., Liu, J., 2016. Inorg. Chem. 55, 8193–8200.
Zhou, W., Saran, R., Liu, J., 2017. Chem. Rev. 117, 8272–8325.